Research on Engineering Structures & Materials
www.jresm.org
MIM Research Group

Research Article

Experimental performance of CFRP strengthened square RC columns with inadequate interior ties: Effects of slenderness and load eccentricity

Ali Majid Mousa [*,a], Salah R. Al Zaidee [b]

Department of Civil Engineering, College of Engineering, University of Baghdad, Baghdad, Iraq

Article Info

Article History:

Received 23 May 2026

Accepted 25 June 2026

Keywords:

CFRP wrapping;
Concentric loading;
Eccentric loading;
Inadequate interior ties;
RC columns;
Slenderness

Abstract

This study investigated the behavior of short and slender square reinforced concrete (RC) columns with inadequate interior ties under concentric and eccentric loading. An eccentricity of 30 mm was adopted to evaluate the influence of load eccentricity on column behavior. Inadequate interior ties refer to insufficient transverse reinforcement provided to laterally support intermediate longitudinal bars. Twelve 1/4-scale square RC columns, comprising six short and six slender specimens, were tested with and without adequate interior ties. Specimens with inadequate interior ties were strengthened using full carbon fiber-reinforced polymer (CFRP) wrapping with a CFRP volumetric ratio of approximately 0.9%. The results showed that inadequate interior ties reduced the axial strength of short columns by approximately 27% under concentric loading, whereas only a marginal reduction of about 1% was observed in slender columns. Brittle failure occurred in both short and slender columns with inadequate interior ties under concentric compression. Under eccentric loading, the corresponding strength reductions were approximately 11% and 4% in the short and slender columns, respectively, indicating a less pronounced influence of inadequate interior ties. Full CFRP wrapping prevented brittle failure and improved the structural performance of the strengthened columns, increasing displacement ductility by up to 22% in short columns and 11% in slender columns. The beneficial effect of CFRP confinement was more pronounced in short columns than in slender columns. These findings demonstrate that CFRP confinement is an effective strengthening technique for square RC columns with inadequate interior ties.

1. Introduction

The basic idea of confining concrete was first proposed by Richart et al. [1], who showed that lateral pressure greatly increases the compressive strength of concrete and alters its stress–strain relationship. Many studies were conducted after this foundational study to examine the influence of transverse reinforcement on confined concrete. Sheikh and Uzumeri [2] conducted an experimental study on tied columns to investigate the effectiveness of transverse reinforcement location. It was concluded that the strength and ductility of confined columns are significantly influenced by tie disposition, spacing, and degree of lateral confinement applied to the concrete core. Subsequently, Mander et al. [3] highlighted the function of lateral transverse reinforcement. The study considered that an effective lateral confining pressure is generated in the column core. The study stated that the behavior of concrete under compression is directly related to the confinement provided by ties. Extending this work, Saatcioglu et al. [4] studied the performance of confined RC columns under eccentric loading. They concluded that when sufficient transverse confinement is provided, a very ductile flexural behavior will be observed.

*Corresponding author: ali.musa2301@coeng.uobaghdad.edu.iq
[a]orcid.org/0009-0001-5966-6232; [b]orcid.org/0000-0002-5867-4193
DOI: http://dx.doi.org/10.17515/resm2026-1702ma0523rs

Several recent studies have investigated the contribution of transverse reinforcement to the confinement of RC columns. For instance, Somma & Pieretto [5] studied confinement of high-strength concrete columns under axial load through a critical review of the adequacy and limitations of international design codes. Ma et al. [6] tested 27 rectangular RC columns with corroded transverse reinforcement and various reinforcement details. The results showed that not only the level of corrosion but also the arrangement of the transverse reinforcement has a substantial effect on both the maximum axial strength and the corresponding response. Benedetti & Bairán [7] investigated rectangular RC columns with limited confinement detailing and considered the effect of insufficient anchorage of transverse reinforcement. The research revealed that insufficient anchorage of the ties reduced the confining pressure in the concrete core, thereby reducing the column's ultimate strength. Insufficient lateral reinforcement can lead to inadequate concrete confinement, thereby reducing the load-carrying capacity and increasing the vulnerability of RC members [8].

Fiber-reinforced polymer (FRP) composites have become widely used in civil engineering applications because of their high performance-to-weight ratio, including superior strength-to-weight and stiffness-to-weight ratios, as well as excellent durability and corrosion resistance [9–13]. These materials are usually available in sheet, strip, and fabric forms and can be widely used for retrofitting and strengthening reinforced concrete (RC) structures. FRP systems have been applied extensively to strengthen RC columns since the mid-1980s because these materials are lightweight, offer high tensile strength, have simple installation procedures, and allow structures to be returned to service quickly after repair. Previous findings indicate that FRP strengthening can restore the column's original capacity in many cases and even increase its overall performance and load-carrying capacity [14–16]. Additionally, using FRP sheets to enhance RC columns has been widely applied in deficient or substandard buildings and bridge systems [17].

Based on fiber type, FRP composites are commonly classified into carbon fiber-reinforced polymers (CFRP), glass fiber-reinforced polymers (GFRP), basalt fiber-reinforced polymers (BFRP), and aramid fiber-reinforced polymers (AFRP) [18,19]. Among these systems, CFRP is one of the most widely used and well-researched composite materials due to its high strength-to-weight ratio, good corrosion resistance, ease of installation, and highly adaptable mechanical properties [20]. Numerous experimental studies have demonstrated that CFRP strengthening can significantly improve the cracking resistance, axial load capacity, and overall structural performance of RC members under both concentric and eccentric loading conditions [21]. Furthermore, CFRP confinement of compression members has demonstrated remarkable efficiency, with many studies reporting an approximately 56% increase in load-carrying capacity relative to unconfined specimens [22].

Many studies have investigated the response of CFRP-strengthened concrete columns under various loading conditions. CFRP has been shown to enhance the structural behavior of short RC columns in previous studies. Mai et al. [23] investigated the behavior of square RC columns externally confined with full and partial CFRP wraps and observed a distinct enhancement in strength and ductility of the confined specimens. Similarly, although Mercimek et al. [24] did not use full CFRP jacketing, their investigation of deficient square RC columns found that CFRP strengthening increased axial load capacity by 53% and improved initial stiffness by approximately 70%.

Previous studies have also confirmed the beneficial effects of CFRP confinement on the structural performance of slender RC columns. Saleh et al. [25] demonstrated that CFRP wrapping of slender RC columns enhanced compressive strength and ductility. In contrast, the same study showed that the effectiveness of CFRP confinement decreases substantially for slender columns compared to short columns. Narule & Bambole [26] also studied CFRP-strengthened slender rectangular RC columns with different slenderness ratios and concluded that slenderness has a significant influence on the ultimate strength, yield strength, and ductility of wrapped columns. In addition, Ali et al. [27] experimentally investigated slender recycled aggregate concrete (RAC) columns confined with CFRP jackets, and their test results indicated that both the lateral reinforcement

arrangement and the amount of CFRP wrapping significantly influenced the columns' load-carrying capacity.

Furthermore, Al-Sherrawi et al. [28] conducted analytical and numerical research on CFRP-strengthened RC columns under axial and eccentric loads. The study observed considerable second-order effects, even with increased axial and flexural capacities resulting from increasing the CFRP reinforcement ratio. Similarly, Mousa & Al Zaidee [29] conducted numerical studies on CFRP-strengthened short and slender RC columns, accounting for geometric imperfections, and found that both the strength and ductility of the columns decreased with increasing imperfection amplitude, regardless of the confinement condition. According to ACI 318-25 [30], intermediate longitudinal bars should be adequately restrained, limiting the clear distance between an unsupported bar and a laterally supported bar to 150 mm. To represent a non-compliant detailing condition, a full-scale RC column that did not satisfy this requirement was selected and subsequently scaled to 1/4 of its original dimensions for experimental testing. This configuration was used to represent RC columns with inadequate lateral restraint of the intermediate longitudinal bars. This condition may arise from outdated detailing practices, construction deficiencies, or insufficient compliance with code provisions.

Numerous studies have investigated the effect of CFRP confinement on RC columns. However, the combined influence of column slenderness and load eccentricity has received relatively little attention, despite its practical importance in RC column design and assessment. Moreover, limited attention has been given to square RC columns with inadequate interior ties, particularly under combined slenderness and eccentric loading, where the effectiveness of CFRP confinement remains insufficiently understood. In addition, the effectiveness of full CFRP wrapping in compensating for inadequate internal confinement in both short and slender columns has not been adequately clarified, despite its potential as a practical strengthening solution for existing RC columns with inadequate interior ties. Accordingly, this study aimed to experimentally investigate the effect of full CFRP wrapping on the structural behavior, axial strength, displacement ductility, strain response, and failure characteristics of short and slender square RC columns with inadequate interior ties under concentric and eccentric compression loading.

2. Specimen Details and Material Properties

2.1. Specimen Details and Labeling

The study utilized one-fourth-scale square RC columns with constant cross-sectional dimensions (140 × 140 mm). The height of the short columns was 750 mm, while a slender column had a height of 1750 mm. As illustrated in Fig. 1, Columns A and B were geometrically identical and shared the same boundary conditions, but differed in the presence or absence of adequate interior ties. A consistent labeling system was adopted to identify the different column configurations and loading conditions. Each specimen designation consists of a three-capital-letter label followed by a suffix (which identifies the column characteristics). The initial letter denotes the slenderness of the column: L for long (slender) columns and S for short ones. The second letter represents the confinement condition: C indicates columns confined with CFRP, and U refers to unconfined columns.

The third letter (for example, A or B) differentiates the reinforcement details between Column A and Column B, as explained previously in Fig. 1. The suffix following the hyphen specifies the scale level and the loading condition (identifying the testing conditions). Here, F refers to full-scale models and S to scaled-down specimens. At the same time, C indicates concentric loading applied with zero eccentricity, and E30 represents eccentric loading applied with an eccentricity (e) of 30 mm. For instance, SCB-SC represents a 1/4-scale short confined type B column under concentric loading, or simply a short column with inadequate interior ties strengthened using full CFRP wrapping under concentric loading. An eccentricity of 30 mm was selected to represent an eccentric loading condition. This value satisfies the condition $0.2h \leq e \leq e_b$, where h is the section dimension perpendicular to the bending axis, and e_b is the balanced eccentricity. This range enabled systematic evaluation of the influence of eccentric loading on column behavior.

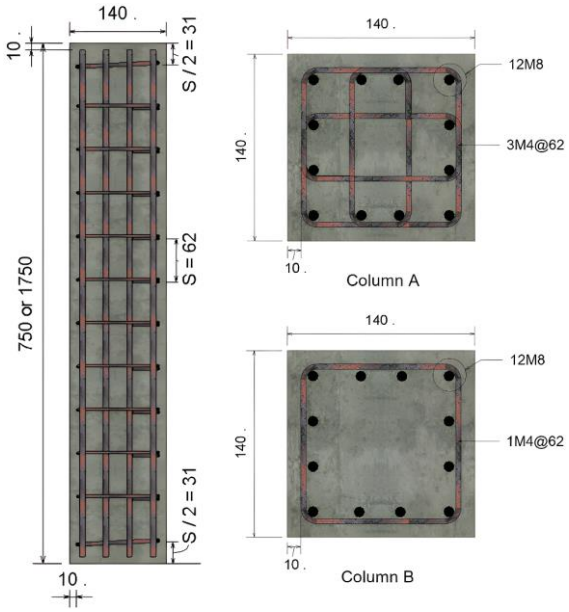

Fig. 1. Geometric details of the 1/4-scale square RC column specimens (all dimensions are in mm)

The slenderness ratio was approximately 18 for the short column specimens with a height of 750 mm. In contrast, the slender column specimens with a height of 1750 mm exhibited a slenderness ratio of approximately 42. The reinforcement details, corresponding to a longitudinal reinforcement ratio of approximately 3%, were scaled from the equivalent full-scale column, which was reinforced with 32 mm-diameter longitudinal bars and 12 mm-diameter ties. Accordingly, 8 mm-diameter longitudinal bars were used in the 1/4-scale specimens to maintain geometric similarity to the prototype. However, 4 mm-diameter ties were adopted instead of the geometrically scaled 3 mm-diameter ties because 3 mm reinforcement bars are not commercially available. In addition, the relatively small bar diameters and the clear spacing between adjacent bars were sufficient to allow proper concrete flow and placement without casting difficulties.

For the strengthened specimens, a corner radius of 25 mm was adopted in the equivalent full-scale columns (560 × 560 mm) prior to CFRP installation. Eight CFRP plies were used, corresponding to a CFRP volumetric ratio of approximately 0.9%. This radius exceeds the minimum corner radii specified by ACI PRC-440.2-23 [31] and the CFRP manufacturer (Fosroc), which recommend minimum values of 13 mm and 10 mm, respectively, to facilitate fiber wrapping and reduce stress concentrations at corner regions. Based on the adopted geometric scale factor of 4, the corners of the 1/4-scale specimens were rounded to an approximate radius of 6.3 mm to represent the 25 mm radius used in the full-scale columns. The 1/4-scale specimens were strengthened using two CFRP plies to maintain approximately the same CFRP volumetric ratio of 0.9%. Therefore, the adopted corner geometry was considered adequate for reducing stress concentrations and promoting effective stress transfer within the CFRP jacket.

In this study, a CFRP volumetric ratio of approximately 0.9% was adopted, as it represents a practical strengthening ratio frequently reported in the literature. The selected ratio also provides effective confinement while remaining practical in both cost and field applications.

2.2. Concrete Compressive Strength

Self-compacting concrete (SCC) was used in this study. The compressive strength of concrete was determined after 28 days of continuous curing by testing three cylindrical specimens (150 × 300 mm) in accordance with ASTM C39/C39M-21 and three cube specimens (150 × 150 × 150 mm) based on BS EN 12390-3:2019. From the cylinder specimens, the average compressive strength was 28.7 MPa, and from the cube specimens, it was 39.5 MPa. However, the cylinder compressive strength of 28.7 MPa was adopted as the concrete compressive strength throughout this study.

The maximum aggregate size used in the concrete was 19 mm. This aggregate size was compatible with the reinforcement arrangement adopted in the specimens, and reinforcement placement and concrete casting were performed without complications.

2.3. Reinforcing Steel Properties

In the present study, tensile tests were conducted on 4 mm and 8 mm diameter reinforcing bars. Three 450 mm specimens of each diameter were tested to determine the steel reinforcement's physical and mechanical characteristics. The steel properties are shown in Table 1.

Table 1. Physical and mechanical properties of reinforcing steel bars

Bar Designation	Nominal Diameter (mm)	Cross-Sectional Area (mm^2)	Yield Strength (MPa)	Tensile Strength (MPa)	Tensile Strength/Yield Strength	Elongation (%)	Reduction of Area (%)	Modulus of Elasticity (GPa)
4	4.06	12.95	539	683	1.27	—	32	200
8	7.97	49.89	440	557	1.27	33	—	200

The 4 mm bars were tested in accordance with ASTM A1064/A1064M-24, and their performance met the strength requirements of ASTM A1064 Grade 77.5. By contrast, the 8 mm bars were tested in accordance with ISO 6935-2, which specifies the mechanical properties and testing requirements for steel reinforcement for concrete. The 8 mm bar specimens met the strength requirements of ISO 6935, Grade B400B-R.

2.4. CFRP Sheets and Epoxy Resin

The RC column specimens were strengthened with CFRP sheets (Nitowrap CWS 300) manufactured by Fosroc [32]. Table 2 shows the mechanical properties of the CFRP material. In addition, a two-component epoxy resin, Sikadur-330, produced by Sika Services AG [33], was used for CFRP strengthening as an adhesive and impregnating agent. In the wet lay-up method, epoxy is used to saturate the CFRP sheets, which are then laid onto the prepared concrete surface to provide sufficient bonding and stress transfer between the CFRP jacket and the concrete substrate.

Table 2. Mechanical properties of the CFRP plies [32].

Product grade	Nitowrap CWS
Fiber density (g/cm^3)	1.8
Fiber area weight (g/m^2)	300
Standard roll width (mm)	500
Standard roll length (m)	100
Design thickness (mm)	0.166
Ultimate elongation or rupture strain	2.1%
Fiber E-modulus (MPa)	230×103
Tensile strength (MPa)	3481

Table 3. Mechanical properties of Sikadur 330 epoxy resin [33]

Property	Value
Modulus of elasticity in flexure	3800 N/mm^2 (7 days at +23 °C)
Tensile strength	30 N/mm^2 (7 days at +23°C)
Modulus of elasticity in tension	4500 N/mm^2 (7 days at +23 °C)
Tensile strain at break	0.9 % (7 days at +23 °C)
Tensile adhesion strength	Concrete fracture (> 4 N/mm2) on sandblasted substrate
Coefficient of thermal expansion	4.5×10^{-5} 1/K (for a temperature range from −10 °C to +40 °C)
Service temperature	−40 °C to +45 °C

The resin components were mixed (A:B=4:1 by weight, according to the manufacturer's recommended ratio) before application. The resin mix exhibits excellent workability and bonds

well to concrete surfaces, making it suitable for manual wrapping and saturating processes. The pot life of the mixed material is about 60 minutes at 23 °C [33]. Based on technical information from the manufacturer, the properties of epoxy resin are given in Table 3. Moreover, CFRP sheets and epoxy resin are illustrated in Fig. 2.

Fig. 2. CFRP strengthening materials and tools: CFRP sheet, epoxy resin, and application rollers

3. Experimental Program and Test Procedure

The experimental program consisted of two main groups of square RC columns: short columns and slender (long) columns. In each group, specimens with adequate interior ties were tested in the unconfined condition, whereas specimens with inadequate interior ties were tested in both unconfined and CFRP-confined conditions using two CFRP plies under concentric (e = 0) and eccentric (e = 30 mm) axial loading. A total of twelve specimens were prepared, including six short columns and six slender columns. In each group, two specimens with adequate interior ties were designated as reference (control) columns. For the short column group, SUA-SC and SUA-SE30 were used as reference specimens for comparison with SUB-SC, SUB-SE30, SCB-SC, and SCB-SE30. Similarly, LUA-SC and LUA-SE30 were used as reference specimens for comparison with LUB-SC, LUB-SE30, LCB-SC, and LCB-SE30 in the slender column group.

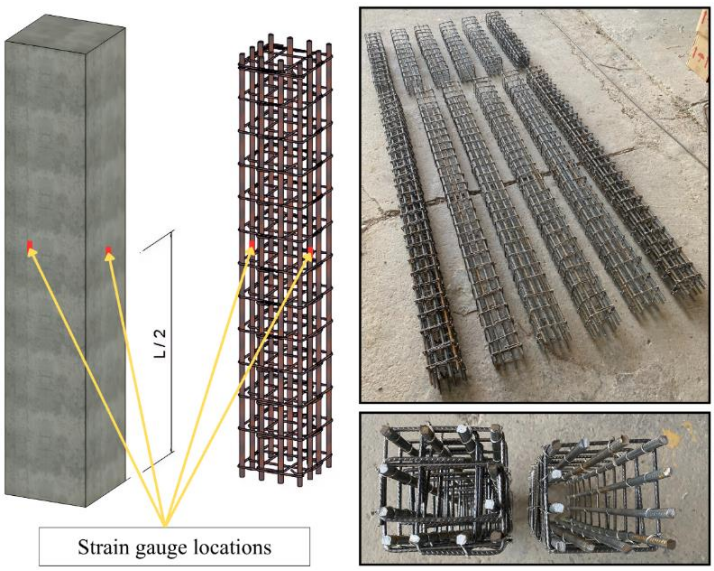

Fig. 3. Steel reinforcement arrangement and strain gauge locations for concrete and steel reinforcement (where L is the column length)

The reinforcement cages for the specimens were fabricated and installed in accordance with Fig. 1. Additionally, four strain gauges were installed on each specimen at the mid-height section, as shown in Fig. 3: two were connected to the concrete to measure the axial strain of the concrete, and

two were bonded to opposite longitudinal reinforcing bars to measure the axial strain in the reinforcing bars that are supported and unsupported with interior ties. Because the column specimens were heavily reinforced (reinforcement ratio of 3%), had a high slenderness ratio, and used interior ties with a geometric reduced-scale factor of 4, they were cast horizontally to avoid potential honeycombing and ensure proper concrete filling around the reinforcement. After demolding, the RC columns were continuously cured for 14 days (see Fig. 4).

Fig. 4. Casting and curing of the specimens

To strengthen the column specimens, the concrete surfaces were mechanically ground with an angle grinder to remove laitance and weak particles. The surface was cleaned with air and water and dried to provide a clean, roughened substrate. Column corners were also rounded with a radius of approximately 6.3 mm to reduce stress concentration. The CFRP installation process is shown in Fig. 5. The wet lay-up technique was applied to strengthen the specimens with CFRP. A two-component epoxy resin (hardener and resin) was mixed at a 1:4 weight ratio and used as a bonding adhesive. The process began with applying a thin coat of epoxy to the concrete. The CFRP sheet was wrapped around the column in the hoop direction. A laminating roller and a corner roller were used to remove entrapped air and ensure proper fiber impregnation.

Fig. 5. CFRP strengthening using the wet lay-up technique

A continuous CFRP jacket with two plies was employed around all four columns (two short and two slender). Another coat of epoxy was applied to the first CFRP layer to ensure a good bond with the second ply. Following wrapping, the outer surface of the CFRP layers was coated with a final epoxy to form a composite system and ensure a full bond between the CFRP jacket and the concrete substrate. For each CFRP layer, an overlap length of 100 mm was used. Moreover, both confined and unconfined column specimens were locally strengthened at the top and bottom ends to avoid premature end crushing. A single CFRP sheet strip was covered at both ends with a width of 100 mm for short columns, and 165 mm for slender columns. The placement of the CFRP strips involved applying epoxy resin both before and after the installation to ensure proper adhesion. The CFRP-wrapped specimens were left to cure at room temperature for 10 days, allowing the epoxy adhesive to cure, as incomplete curing could significantly affect test results. The mechanical properties of

the epoxy are typically reported after 7 days at 23 °C according to the manufacturer. All RC column specimens, both short and slender, were tested under axial compression using a hydraulic compression testing machine (CTM) after 28 days of casting. Custom-fabricated steel loading heads (caps) were installed at both ends of the columns to ensure proper load transfer and uniform stress distribution. Loading heads for both concentric and eccentric axial load applications were designed to control the position of the applied loads relative to the centroidal axis of the column cross-section. In addition, the loading system was configured to simulate pinned–pinned boundary conditions through the hinged-end connections integrated into the steel loading heads. Fig. 6 shows the detailed configuration of loading heads.

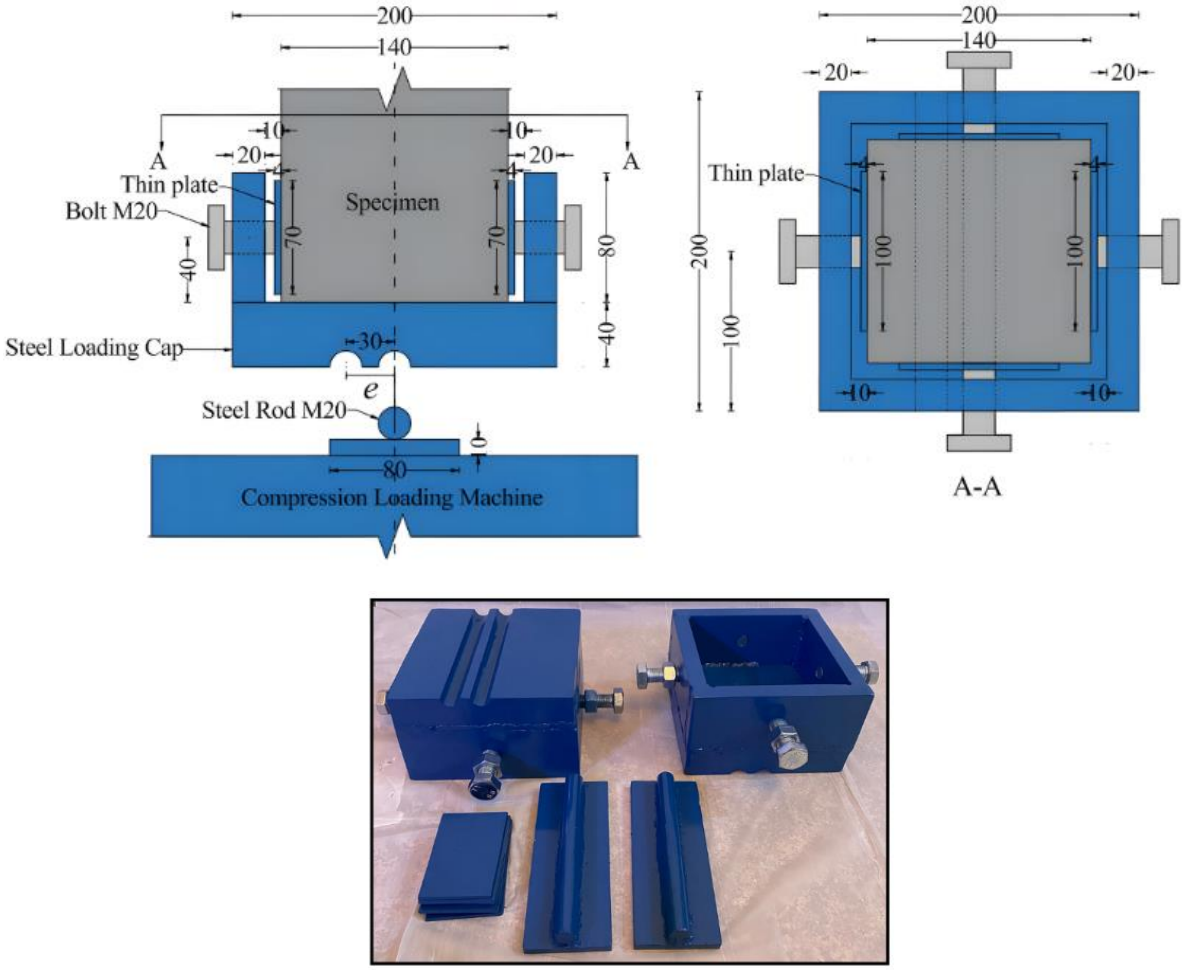

Fig. 6. Details of the custom-fabricated steel loading caps used in the experimental setup (all dimensions are in mm)

A hydraulic compression testing machine (CTM), a 200-ton load cell, linear variable differential transducers (LVDTs), and strain gauges were used as part of the measurement system in the test setup. In this test, a hydraulic jack was used to apply the load to the column from the bottom to the top. To measure the applied loads, a load cell was installed between the loading head and the hydraulic jack. The column axial displacement of the tested specimens was recorded using a single LVDT fixed at a point on the lower frame support. To measure lateral displacement during the test, two LVDTs were attached at mid-height, facing each other, on both sides of the test specimens. Furthermore, a laser level was used to ensure proper alignment and prevent unintended deviation during loading. This process was repeated for all RC column specimens with concentric and eccentric loading. A similar arrangement of strain gauges was also installed on the concrete at mid-height of the specimens, as previously described in Fig. 3. Fig. 7 shows the final test setup with the measurement devices. Before commencing each test, a small seating load was applied to ensure proper seating and alignment of the specimen within the test setup. Subsequently, all measuring devices were reset to zero before data acquisition began. The specimens were then subjected to

monotonic axial compression under gradually applied loading, and the tests were continued beyond the peak load whenever possible to capture the post-peak response. During testing, the applied load, displacements, and strains were continuously recorded using the data logger.

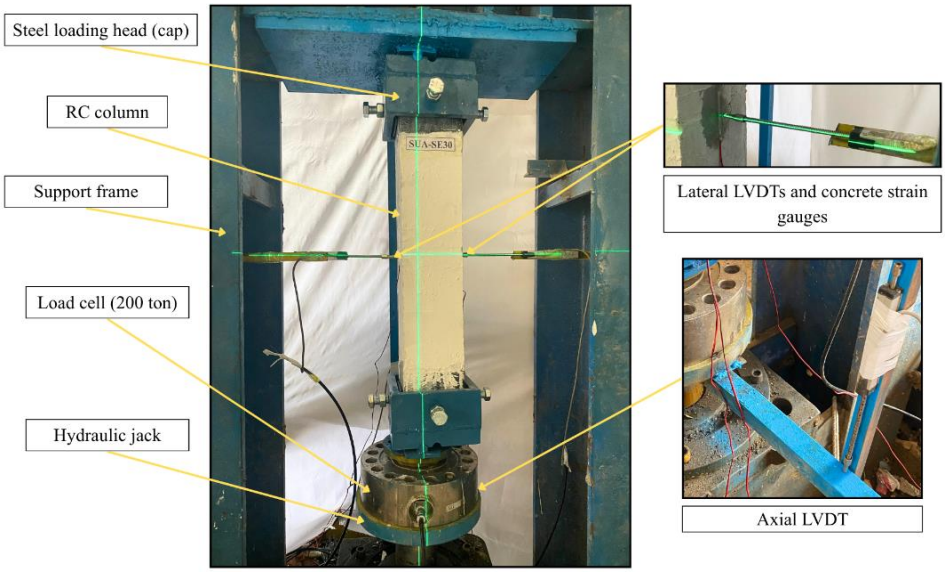

Fig. 7. Final test setup of RC column specimens with measurement devices

4. Experimental Results and Discussion

4.1. Axial Load–Displacement Behavior

Fig. 8 shows the axial load–axial displacement curves for all short and slender square RC column specimens. Structural performance assessment was based mainly on the axial response to concentric loading, since axial deformation governs the behavior of the structure under concentric compression. As illustrated in Fig. 8(a) for short columns under concentric axial loading, the maximum (peak) axial load decreased from 1049 kN, for the reference specimen SUA-SC, to 766 kN in the specimen with inadequate interior ties (SUB-SC), representing a reduction of approximately 27%. Similarly, the axial displacement at peak load decreased from 3.05 mm to 2.35 mm, corresponding to a reduction of about 23%.

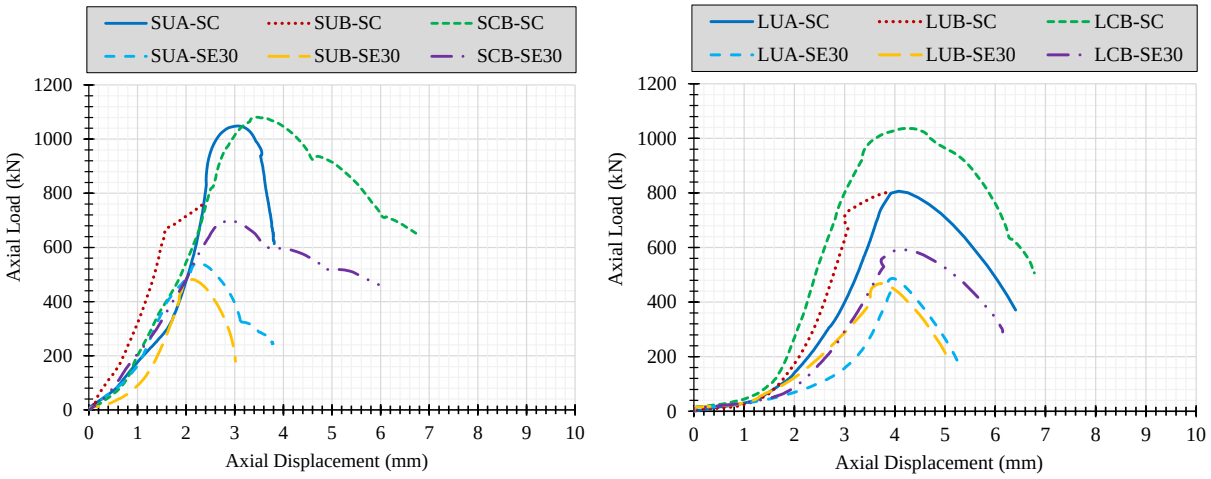

Fig 8. Axial load–axial displacement behavior for RC column specimens: (a) short columns and (b) slender columns

These reductions reflect that the longitudinal reinforcement and concrete core were less confined and laterally restrained due to inadequate interior ties, thus leading to degradation of the axial load capacity and axial deformation response. In addition, the deficient specimen failed suddenly in a brittle manner immediately upon reaching the peak load, indicating the limited confinement capacity of the concrete core. In comparison, the specimen with insufficient interior ties enhanced by two plies of fully wrapped CFRP (SCB-SC) achieved a maximum axial load of 1081 kN, and a peak load axial displacement of 3.45 mm, which was approximately a 3% increase in peak axial load and nearly 13% increase in peak axial displacement compared to the reference specimen. These findings demonstrate that CFRP confinement compensated for the inadequacy of internal ties by increasing load-carrying and deformation capacities under concentric compression, and preventing brittle failure. For short columns with eccentric axial loading, the maximum axial load was reduced from 544 kN in the reference specimen SUA-SE30 to only 482 kN in SUB-SE30, corresponding to an 11% decrease due to insufficient interior ties. Additionally, the axial displacement at peak load decreased from 2.25 mm to 2.13 mm, corresponding to approximately a 5% decrease. When under eccentric loading conditions, the effects of insufficient interior ties on both axial load capacity and deformation response were less severe than in concentrically loaded short columns, with no brittle failure observed in either specimen. This behavior was primarily attributable to eccentric loads and flexural action, which reduced the confinement effect of the interior ties.

On the other hand, column performance improved significantly when two plies of fully wrapped CFRP were used to strengthen the specimen with insufficient interior ties (SCB-SE30). The strengthened specimen attained a peak load of 699 kN and an axial displacement at this load equal to 2.85 mm, improving by approximately 29% in peak axial load as well as 27% in axial displacement over the corresponding reference specimen (SUA-SE30). These results suggest that full CFRP wrapping effectively improved the load-carrying and deformation capacities of short columns under eccentric axial loading. As shown in Fig. 8(b), the peak axial load of slender columns under concentric axial loading decreased only slightly from 806 kN for the reference specimen (LUA-SC) to 802 kN for a specimen with inadequate interior ties (LUB-SC), representing a difference of less than 1%. In the same manner, the axial displacement at maximum load was reduced from 4.08 mm to 3.85 mm, which represents a reduction of approximately 6%. While inadequate interior ties had only a minimal effect on the peak axial load and deformation capacity, the deficient specimen failed in a brittle manner before reaching its peak load. This observation indicates that interior ties improve confinement conditions and post-peak performance of slender columns under concentric compression. According to Wight [34], slender columns experience a reduction in axial-load capacity due to moments generated by lateral deflections. Therefore, the behavior of the slender specimens was mainly governed by stability-related effects rather than by confinement efficiency, thereby reducing the apparent influence of inadequate interior ties on the peak load. Nevertheless, brittle failure was observed, indicating that inadequate interior ties continued to influence the specimens' failure behavior.

By wrapping the deficient slender column (LCB-SC) with a full CFRP jacket, the column's performance increased significantly. The peak axial load increased to 1037 kN, corresponding to an approximate 29% increase compared with the reference specimen (LUA-SC); on the other hand, the axial deformation at peak load increased by about 4%, reaching a value equal to 4.25 mm. In addition, no brittle failure was observed in the strengthened specimen, which can be attributed to the increased confinement condition and improved overall performance of the slender column under concentric compression. For slender columns subjected to eccentric axial loading, the maximum axial load decreased from 487 kN in the reference specimen (LUA-SE30) to 468 kN in the specimen with inadequate interior ties (LUB-SE30), with a 4% reduction in peak load. Correspondingly, at peak load, the axial displacement was reduced from 3.95 mm to 3.73 mm, a reduction of approximately 6%, with no brittle failure in either specimen. The results show that the inadequate interior ties had relatively little effect on both the strength and the deformation capacity of a slender column subjected to axial eccentric loading.

In strengthening the deficient slender column (LCB-SE30), applying CFRP wrapping increased the load-carrying capacity and marginally improved the deformation capacity. The maximum value of

axial load increased to 592 kN with an increase of approximately 22% compared to the reference specimen (LUA-SE30). In contrast, the axial displacement at peak load increased slightly to 4.16 mm with an improvement of around 5%. However, for the slender columns, the marginal gains in deformation capacity were less than those from strengthened short columns under the same eccentric loading condition. This behavior was primarily linked to a greater impact of slenderness and flexural instability on the reduction in CFRP-confinement effectiveness in deformation capacity. Nevertheless, the CFRP wrapping was still successful in improving the entire behavior of slender columns subjected to eccentric axial load. On the other hand, since load eccentricity and second-order effects significantly affect the overall column behavior, only eccentrically loaded columns were evaluated for lateral deformation response, as shown in Fig. 9.

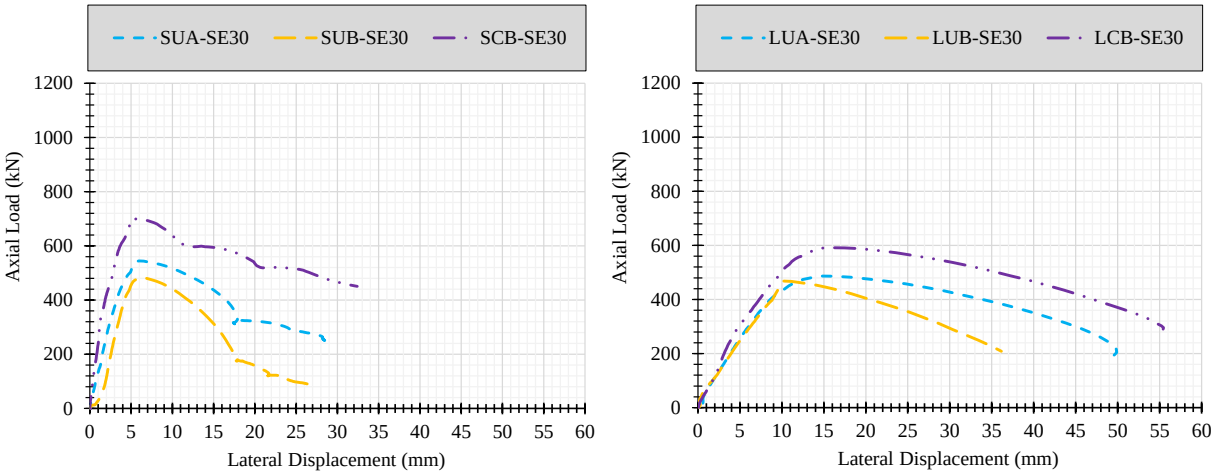

(a) (b)

Fig 9. Axial load– lateral displacement behavior RC column specimens: (a) short columns and (b) slender columns

Besides the axial response, the lateral deformation behavior of eccentrically loaded columns was also assessed. Fig. 9(a) shows that the short columns showed only limited variation in lateral deformation response. The lateral displacement at peak load of the reference specimen (SUA-SE30) was 5.97 mm, while in the specimen without sufficient interior ties (SUB-SE30), that value reached 6.32 mm, representing an increase of approximately 6%. On the other hand, a lateral displacement of 5.58 mm was observed in specimen SCB-SE30 strengthened with CFRP sheets, a reduction of approximately 7% compared with the reference specimen. These results show that inadequate interior ties had only a minor effect on the lateral deformation response of the short columns. In contrast, CFRP wrapping retained a level of lateral deformation response close to that of the reference specimen.

Under the same eccentric loading condition, the lateral deformation response of the slender columns was more pronounced than that of the short columns. The lateral displacement at peak load of the reference slender (LUA-SE30) specimen showed a value of 14.42 mm, as also shown in Fig. 9(b), being substantially higher than that corresponding to short columns, indicating that slenderness tends to contribute significantly under eccentric loading. Additionally, the specimen with inadequate internal ties (LUB-SE30) reduced the lateral displacement to 10.12 mm, reflecting a decrease of about 30%. On the other hand, the resulting lateral displacement of the CFRP-confined specimen (LCB-SE30) was 15.70 mm, which is approximately 9% higher than that of the reference specimen. In general, the lateral deformation response of slender columns was primarily governed by slenderness effects that prevailed in the lateral deformation response of slender columns under eccentric loading. Despite the increase in load-carrying capacity of specimen LCB-SE30 due to CFRP confinement, substantial lateral displacement was still observed. The relatively large lateral displacement indicates that slenderness-related deformation and stability effects remained significant in the eccentrically loaded slender column despite the increase in strength.

4.2. Failure Modes of the Tested RC Column Specimens

The failure modes of the tested RC column specimens were observed and documented during the experimental program. The behavior depended on the loading condition, column slenderness, internal confinement (adequate or inadequate interior ties), and CFRP confinement. The failure modes of all specimens are shown in Fig. 10 for the short columns and Fig. 11 for the slender columns. Under concentric loading, both short and slender columns with adequate interior ties (SUA-SC and LUA-SC) failed, with concrete spalling as the main failure mode. At the same time, the longitudinal reinforcement yielded, and the transverse reinforcement remained intact. On the other hand, short and slender specimens with inadequate interior ties (SUB-SC and LUB-SC) failed due to localized concrete crushing, local buckling of longitudinal bars, and rupture of some transverse reinforcement within the failure zone. In addition to providing concrete confinement, the ties act as lateral supports for the longitudinal reinforcement [3,30]. As a result, the absence of adequate interior ties reduced the lateral support of the longitudinal bars, making them more susceptible to local buckling under compressive loading. This behavior was observed in specimens SUB-SC and LUB-SC after failure.

For short and slender specimens with CFRP confinement (SCB-SC and LCB-SC), the overall performance was substantially improved, with no brittle failure, reduced spalling, and greater structural integrity. Rupture of the CFRP sheets occurred primarily in the hoop direction, indicating that the external confinement system failed at its maximum capacity. Under eccentric loading, the short, slender specimens with adequate interior ties (SUA-SE30 and LUA-SE30) failed with concrete spalling on the compression side and cracking on the tension side. The longitudinal steel bars for both specimens yielded. The slender specimen showed greater lateral deformation than the short specimen, indicating the onset of geometric nonlinearity. Furthermore, the transverse reinforcement in both columns was still intact, and the failure occurred approximately at the mid-height of the RC column specimens.

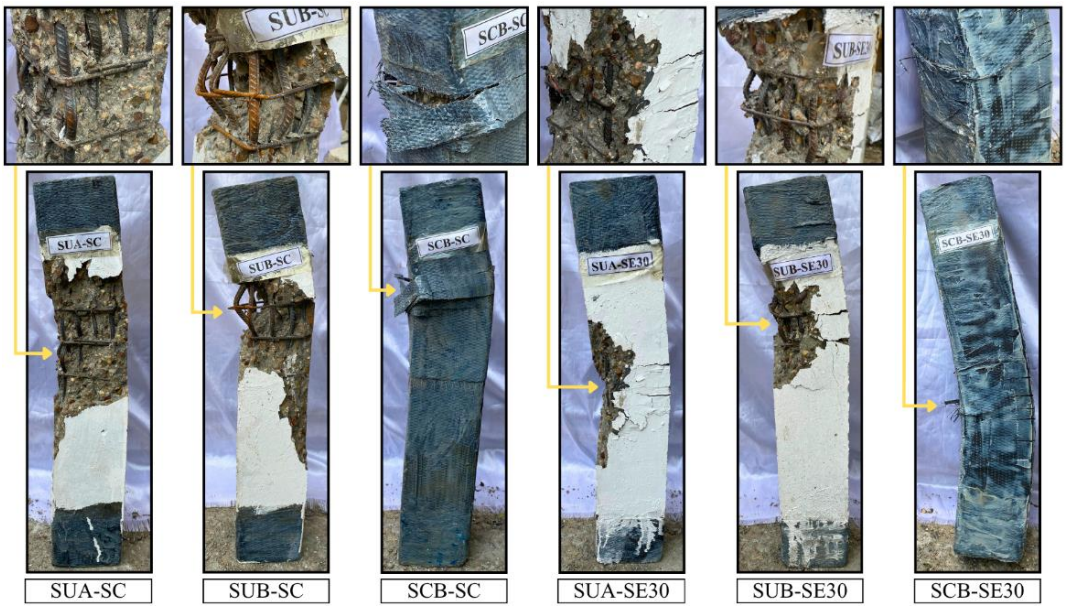

Fig. 10. Failure modes of short RC column specimens

The corresponding specimens with inadequate interior ties (SUB-SE30 and LUB-SE30) failed with concrete spalling on the compression side and cracking on the tension side. The short specimen failed due to yielding and local buckling of the steel bars, whereas the slender specimen failed due to global buckling. Visual inspection indicates that the transverse reinforcement for the short column yielded at the failure zone, while the transverse reinforcement in the slender column was still intact at the failure zone. The failure occurred approximately at mid-height in both RC column specimens. The short column (SCB-SE30) exhibited less spalling and better structural integrity than the unconfined specimens. The CFRP sheets ruptured primarily in the hoop direction at the compression side of the concrete member, with localized rupture on the tension side. Additionally,

the column exhibited yielding failure, indicating a more stable structural response. The CFRP-confined slender column (LCB-SE30) experienced a more pronounced global buckling mode, characterized by substantial lateral curvature resulting from the combined effects of load eccentricity and slenderness. No clear CFRP rupture of the compression face was observed; however, localized rupture was observed on the tension side at mid-height in the column.

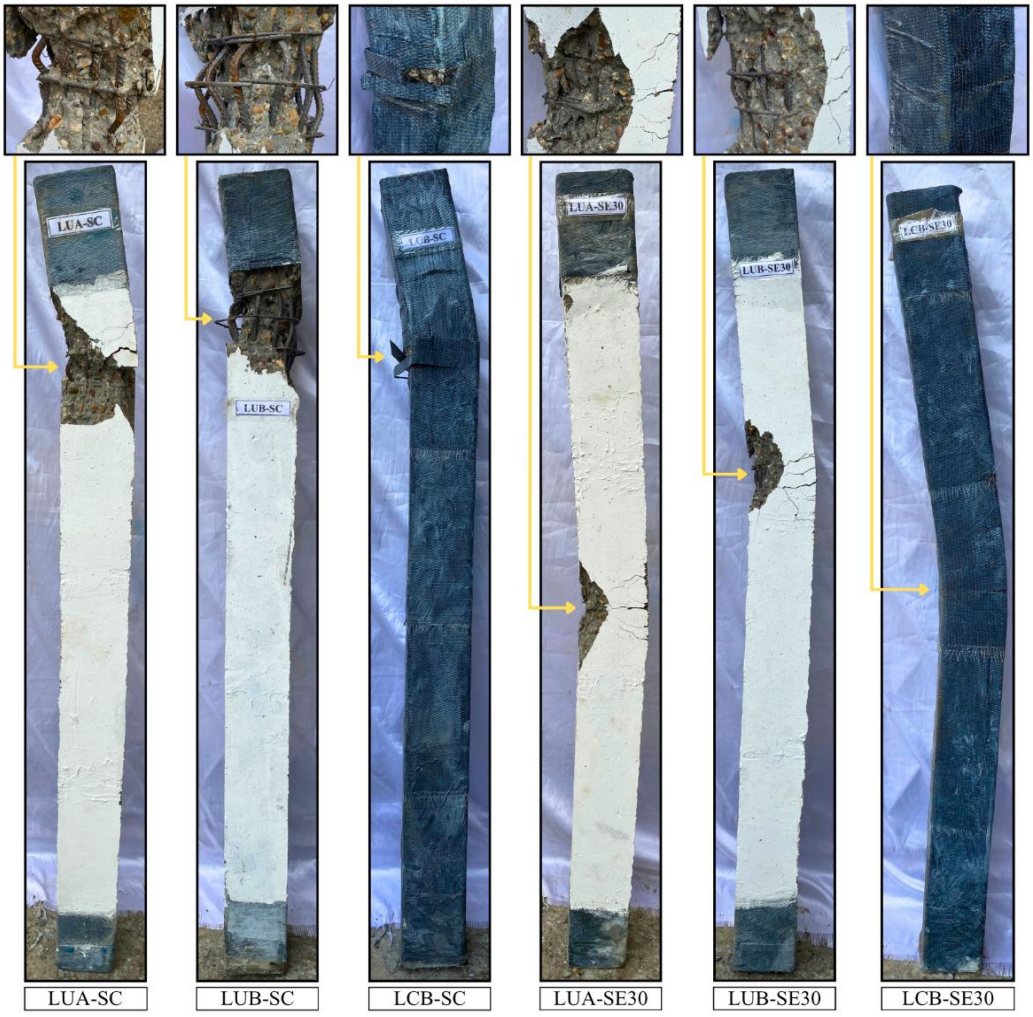

Fig. 11. Failure modes of slender RC column specimens

4.3. Axial Load–Axial Strain Behavior

According to Darwin & Dolan [35], concrete fails in compression by crushing at a strain value of approximately 0.003 and reaches its maximum stress from about 0.002 to 0.003 in this strain range. In contrast, steel reinforcement is commonly assumed to exhibit a sharp yielding behavior. Based on the experimentally obtained yield strength of the steel bars (440 MPa) and their modulus of elasticity (200000 MPa), the corresponding yield strain was approximately 0.0022. Figs. 12-13 illustrate the axial load–axial strain behavior of concrete and the axial load–axial strain behavior of steel reinforcement for all specimens at mid-height, respectively. Positive values in these figures reflect tensile strains, while negative values denote compressive strains. The reported values are the concrete compressive strain and the strains in longitudinal steel bars in both compression and tension. These strain values were reported at the maximum axial load for each specimen.

In the short columns under concentric loading, the concrete compressive strain of reference specimen SUA-SC with adequate interior ties reached 0.0019 at peak load, which was on the lower limit of the range of commonly reported peak concrete strains (0.002–0.003). In contrast, for the specimen with inadequate interior ties (SUB-SC), a low strain of 0.0016 was observed, associated with the comparatively lower confinement provided by the interior ties. Although the failure of

SUB-SC was sudden and severe, its compressive strain never exceeded 0.003, a typical strain for concrete crushing, indicating premature crushing due to insufficient confinement. On the other hand, the specimen confined with CFRP (SCB-SC) exhibited a compressive strain of 0.0029, which is within the typical range for unconfined concrete, showing that fully wrapping CFRP can effectively provide external confinement and improve the strain capacity under concentric compression.

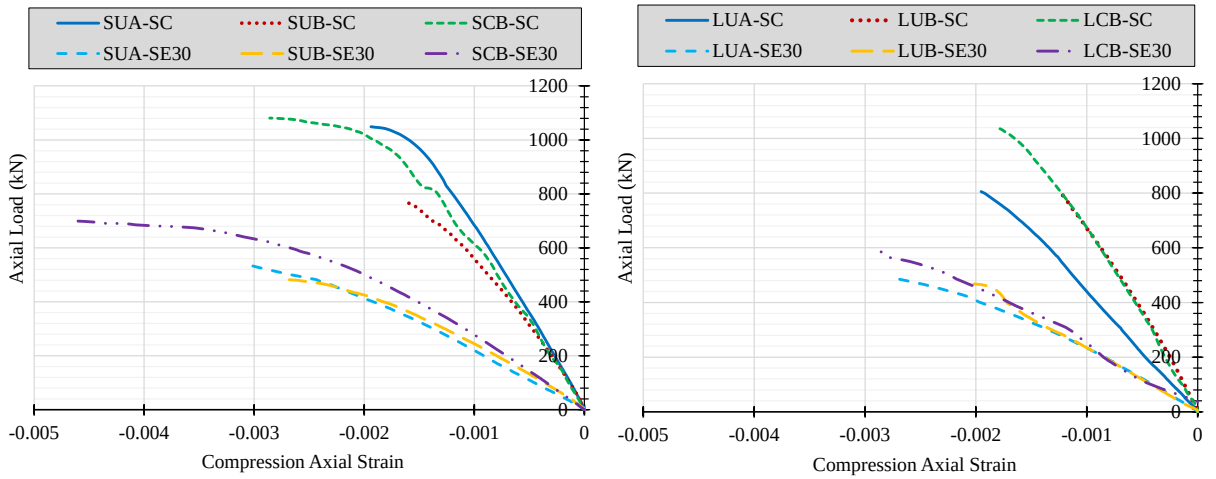

(a) (b)

Fig. 12. Axial load–axial compressive strain behavior of concrete at mid-height: (a) short columns; (b) slender columns

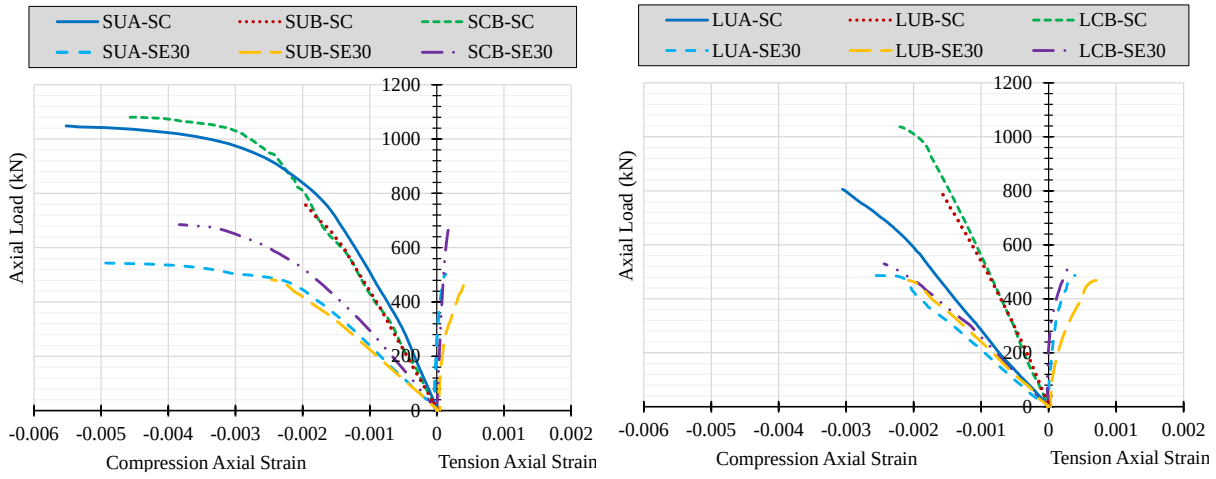

(a) (b)

Fig. 13. Axial load–axial strain behavior of steel reinforcement at mid-height: (a) short columns; (b) slender columns

Under eccentric loading, the concrete compressive strain in the reference specimen (SUA-SE30) reached 0.0031, whereas this value slightly decreased to 0.0027 in the specimen with insufficient interior ties (SUB-SE30). The two values were either within or close to the commonly reported peak concrete strain range. The larger strain recorded in SUA-SE30 was attributed to the better confinement provided by the adequate interior ties. However, the specimen with insufficient interior ties (SCB-SE30) exhibited a high compressive strain of 0.0046 in the concrete under eccentric loading. This compressive strain was compensated for by external CFRP confinement, resulting in a significant increase in strain capacity. The strain response of the slender columns differed from that observed for the short columns due to slenderness. For concentric loading, the concrete compressive strain at peak load was 0.002 in the reference specimen (LUA-SC), within the commonly reported range of 0.002–0.003 for peak concrete strain at failure. In contrast, for the

specimen with insufficient interior ties (LUB-SC), the strain decreased significantly to 0.0012, indicating that inadequate confinement provided by the interior ties had a significant impact. Lower strain was observed in specimen LUB-SC due to insufficient concentric compression capability and rapid failure.

The concrete compressive strain in the CFRP-wrapped specimen (LCB-SC) exceeded 0.0018, which was clearly higher than that in LUB-SC. Despite a slightly lower recorded strain than that of the reference specimen (LUA-SC), the CFRP-confined column displayed a significantly higher axial load capacity. This behavior demonstrates the effect of external CFRP confinement on the structural response of a slender column under concentric compression. Under eccentric loading, in the reference slender specimen (LUA-SE30), at peak load, the concrete compressive strain reached 0.0027, which was within the range often reported for peak concrete strain of 0.002–0.003. Conversely, in the specimen with inadequate interior ties (LUB-SE30), the recorded strain was 0.0020 due to the lower confinement provided by the interior ties. At the same time, it remained at a value close to the lower limit of the average peak strain range. However, for the slender specimen strengthened with CFRP (LCB-SE30), the concrete compressive strain increased to 0.0029, with a slight improvement in strain capacity compared with the reference slender specimen.

The increase in concrete strain due to CFRP confinement was more pronounced in the short columns than in the slender columns. This observation suggests that slenderness-related deformation and stability effects reduced the apparent contribution of CFRP confinement to the measured concrete strain. A similar trend was reported by Saleh et al. [25], who found that the effectiveness of CFRP confinement decreases with increasing column slenderness. The steel strain response was studied under both compressive and tensile loading conditions. For short and slender columns under concentric loading, the columns remained primarily in compression because of the absence of bending effects. In contrast, both compressive and tensile steel strains developed in the eccentrically loaded columns due to the combined axial load and bending effects. However, the tensile steel strain was always smaller than the yield strain, indicating that yielding occurred primarily in the compression reinforcement. This response was attributed to greater stress redistribution and dominant flexural behavior under eccentric loading of the columns.

Under concentric loading, in the reference short specimen (SUA-SC), at peak load, the steel compressive strain reached 0.0055, which was greater than the approximate steel yield strain of 0.0022, indicating yielding of the compression reinforcement. Additionally, the strain decreased significantly to 0.0020 in the specimen with insufficient interior ties (SUB-SC). This reduction highlights the influence of the reduced confinement provided by the interior ties relative to the reference specimen and indicates a lower compression strain capacity. Furthermore, the CFRP-confined specimen (SCB-SC) exhibited a compressive steel strain of 0.0046, indicating that the steel bars in compression yielded. The measured strain was lower than that of the reference column (SUA-SC) even though the axial loading capacity of the strengthened column was higher under concentric compression. Under eccentric loading, compressive steel strain in the reference specimen (SUA-SE30) was 0.0050, which was well above the steel yield strain of about 0.0022 and indicated that compression reinforcement had yielded. In contrast, the compressive strain decreased to 0.0025 in the specimen with inadequate interior ties (SUB-SE30) due to the reduced confinement from fewer interior ties within the concrete core. Moreover, the compressive steel strain at crushing in the CFRP-confined specimen (SCB-SE30) showed a value of 0.0038, which also led to exceeding the yield strain and confirmation of yielding for the compression reinforcement. The achieved strain was lower than that of the reference specimen. However, under eccentric compression, the strengthened column sustained a higher axial load, demonstrating the contribution of external CFRP confinement to the global performance.

In slender columns under concentric loading, an ultimate compressive steel strain of 0.0031 was found in the reference specimen (LUA-SC) at peak load, which was greater than the steel yield strain of approximately 0.0022, indicating yielding of the compression reinforcement. In contrast, the strain decreased to 0.0016 in the specimen with insufficient interior ties (LUB-SC), remaining below the yield strain due to the low confinement provided by the interior ties. The compressive steel strain for the CFRP-confined specimen (LCB-SC) reached a value of 0.0022, which is almost

equal to the steel yield strain. As a result, the recorded strain was partially lower than that of the reference specimen; however, under concentric compression, the axial load was higher for the strengthened column, indicating that external CFRP confinement improves overall structural performance. In addition, slender columns were observed to exhibit similar trends under eccentric loading. The compressive steel strain reached 0.0026 in the reference specimen (LUA-SE30) and decreased slightly to 0.0021 in the specimen with insufficient interior ties (LUB-SE30). However, a compressive steel strain of 0.0024 was recorded for the CFRP-confined specimen (LCB-SE30), indicating partial recovery of the steel strain response relative to the deficient specimen. While the recorded strain was still less than that of the reference specimen, the axial load capacity of this strengthened column under eccentric loading is higher. Overall, observed strains during eccentric loading were within or close to the steel yield strain range. Although a similar trend was observed in compressive steel strain between short and slender columns, the short columns exhibited a higher compressive strain than the slender ones, suggesting the influence of increased slenderness.

4.4. Ductility Behavior

The displacement ductility (μ) of the tested specimens is defined as the ratio of failure displacement (Δ_f), which is obtained at 85% of the peak axial load ($0.85P_u$) on the descending branch of the axial load–axial displacement curve, to the ultimate displacement (Δ_u) at peak axial load, following Ghoroubi et al. [36], as illustrated in Fig. 14.

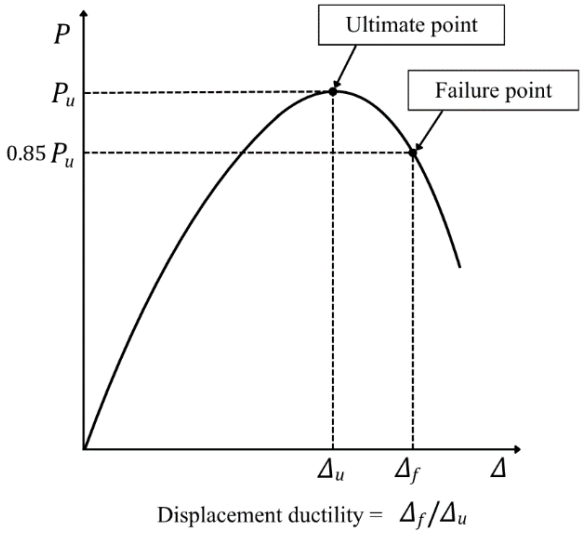

Fig. 14. Definition of the displacement ductility parameters from the axial load–axial displacement curve

The displacement ductility was taken as 1.0 for the concentrically loaded specimens SUB-SC and LUB-SC due to the sudden brittle failure observed at peak load, which prevented the development of a distinct post-peak response. Accordingly, Δ_f was taken equal to Δ_u. The displacement ductility of the reference short specimen (SUA-SC) under concentric loading was 1.18. At the same time, the specimen with inadequate interior ties (SUB-SC) exhibited brittle failure, and thus, no ductility could be determined. Moreover, the specimen confined with CFRP and inadequate interior ties (SCB-SC) showed a ductility index of 1.44; this value was approximately 22% higher than that of its corresponding reference specimen. These results suggest that ductility improved and brittle failure was avoided due to CFRP wrapping, which compensated for the low or nonexistent confinement provided by inadequate interior ties under concentric compression.

The displacement ductility of the reference specimen (SUA-SE30) was 1.23, and the ductility index slightly decreased in the specimen with insufficient interior ties (SUB-SE30) to 1.20, about 2% reduction under eccentric loading. This result shows that insufficient interior ties had a minor effect on the ductility response to eccentric loading. CFRP-confined specimen with insufficient interior ties (SCB-SE30) exhibited improved ductility at failure relative to its reference, with a ductility index of 1.42, an increase of approximately 16%. These results confirm that CFRP

wrapping improved both ductility and overall structural performance under eccentric compression.

The reference specimen with slender columns under concentric loading (LUA-SC) had a displacement ductility of 1.26. In contrast, the specimen with inadequate interior ties (LUB-SC) exhibited brittle failure, and the displacement ductility was not applicable. By comparison, the specimen confined with CFRP and inadequate interior ties (LCB-SC) exhibited a ductility index of 1.31, approximately a 4% improvement compared with the reference specimen. These results suggest that CFRP wrapping improved the slender columns' ductility index and prevented brittle failure under concentric compression. Despite the limited enhancement in ductility, a much higher axial load capacity was achieved with the strengthened column compared to that of the reference specimen. In addition, the displacement ductility index of the reference specimen (LUA-SE30) was 1.12, and the ductility index of the specimen with insufficient interior ties (LUB-SE30) was 1.14. The relatively small difference between these values for the two specimens indicates that inadequate interior ties had only a slight effect on the ductility response of slender columns under eccentric loading. In contrast, specimen LCB-SE30, with inadequate interior ties but confined by CFRP, exhibited greater ductility, with a ductility index of 1.24, approximately 11% higher than that of the corresponding reference specimen. These results confirm that CFRP wrapping improved ductility and enhanced deformation capacity under eccentric loading. A summary of the main experimental results for the tested specimens is shown in Table 4.

Table 4. Experimental results summary of all tested RC columns.

Specimen	Column Type	P_u (kN)	Δ_u (mm)	Δ_f (mm)	Δ_ℓ (mm)	μ	Tensile Steel Strain at P_u	Compressive Steel Strain at P_u	Compressive Concrete Strain at P_u
SUA-SC	Short	1049	3.05	3.60	—	1.18	—	0.0055	0.0019
SUB-SC	Short	766	2.35	2.35	—	1.00	—	0.0020	0.001**6**
SCB-SC	Short	1081	3.45	4.96	—	1.44	—	0.0046	0.0029
SUA-SE30	Short	544	2.25	2.77	5.97	1.23	0.0001	0.0050	0.0031
SUB-SE30	Short	482	2.13	2.56	6.32	1.20	0.000**5**	0.0025	0.002**7**
SCB-SE30	Short	699	2.85	4.06	5.58	1.42	0.0002	0.0038	0.0046
LUA-SC	Slender	806	4.08	5.15	—	1.26	—	0.0031	0.0020
LUB-SC	Slender	802	3.85	3.85	—	1.00	—	0.0016	0.0012
LCB-SC	Slender	1037	4.25	5.57	—	1.31	—	0.0022	0.0018
LUA-SE30	Slender	487	3.95	4.41	14.42	1.12	0.0004	0.0026	0.0027
LUB-SE30	Slender	468	3.73	4.27	10.12	1.14	0.0007	0.0021	0.0020
LCB-SE30	Slender	592	4.16	5.16	15.70	1.24	0.0003	0.0024	0.0029

Note: Δ_ℓ: The lateral displacement at peak axial load.

4.5. Influence of Slenderness and Load Eccentricity on Axial Load Capacity

To investigate the effect of slenderness on axial load capacity, the maximum axial loads of both short and slender columns were compared under similar loading and strengthening conditions, as shown in Fig. 15. Depending on the confinement condition and the type of loading, the impact of slenderness on axial load capacity varied. With increasing slenderness, the reference specimen with adequate interior ties under concentric axial loading (LUA-SC) exhibited approximately a 23% reduction in axial load capacity compared with SUA-SC. Conversely, the specimen with inadequate interior ties (LUB-SC) showed a small variation of approximately 5% as slenderness increased compared with SUB-SC. Additionally, for the specimen with inadequate interior ties and fully wrapped with CFRP (LCB-SC), a minor reduction of approximately 4% in axial load capacity was observed under concentric compression compared with SCB-SC.

Moreover, the slender specimen with adequate interior ties (LUA-SE30) exhibited an approximately 11% reduction in axial load capacity with increased slenderness under eccentric axial loading compared with SUA-SE30. The specimen with insufficient interior ties (LUB-SE30) showed only a 3% reduction compared with SUB-SE30. However, the specimen with inadequate interior ties and fully wrapped with CFRP subjected to eccentric compression (LCB-SE30) showed

a 15% decrease in axial load capacity as slenderness increased compared with SCB-SE30. The results indicate that the effect of increasing slenderness was more pronounced in the CFRP-strengthened column under eccentric loading.

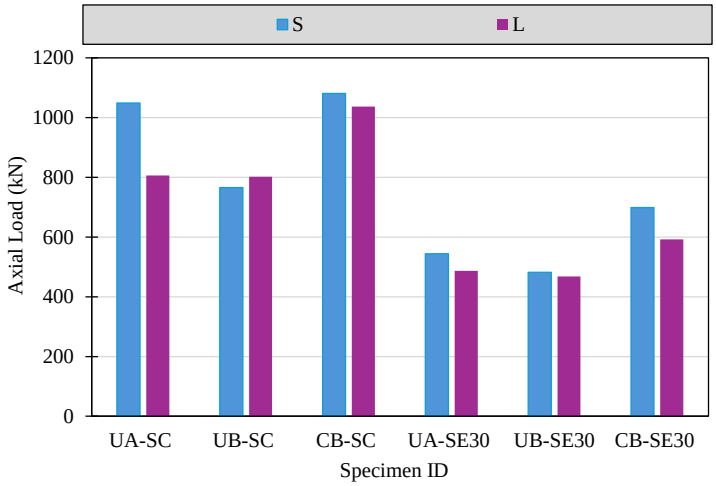

Fig. 15. Effect of slenderness ratio on the axial load capacity of the tested short and slender RC columns under different loading conditions

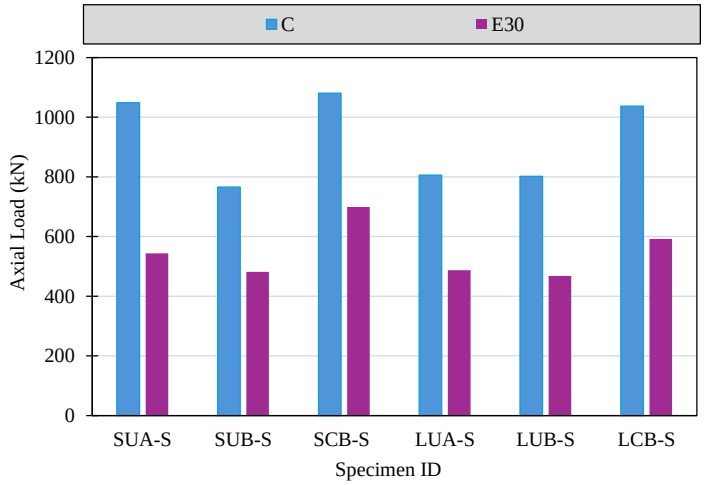

Fig. 16. Effect of load eccentricity on the axial load capacity of the tested short and slender RC columns

The effect of load eccentricity on axial load capacity was investigated by comparing the peak axial loads of concentrically and eccentrically loaded columns with the same confinement and strengthening conditions, as shown in Fig. 16. In the short columns, the adequate interior ties column tested under eccentric loading (SUA-SE30) showed about a 48% decrease in axial load capacity compared to the reference column with concentric loading (SUA-SC). Additionally, the specimen with inadequate interior ties (SUB-SE30) showed a decrease of approximately 37% compared with SUB-SC. In contrast, the CFRP-confined specimen with inadequate internal ties (SCB-SE30) showed about 35% reduction in eccentric loading compared with SCB-SC. These results demonstrate that load eccentricity has a pronounced impact on the axial load capacity of all the short column specimens, regardless of the confinement condition. However, the lower percentage reduction in the CFRP-confined specimen indicated that the adverse effect of load eccentricity on axial load capacity was partially mitigated by CFRP confinement.

In addition, for the case of the slender columns, the specimen with adequate interior ties (LUA-SE30) achieved an approximately 40% decrease in axial load capacity, which was due to increased load eccentricity compared to its preference concentrically loaded specimen (LUA-SC). Similarly, the specimen with inadequate interior ties (LUB-SE30) had a reduction of about 42% in axial load

capacity compared to LUB-SC, and the CFRP-confined specimen with inadequate interior ties (LCB-SE30) exhibited a 43% reduction in axial load capacity when loaded eccentrically compared to LCB-SC. The results indicated that load eccentricity had a pronounced effect on the axial load capacity of slender columns, irrespective of their confinement condition.

5. Conclusions

The results of the tested specimens showed that the response of both short and slender square RC columns with inadequate interior ties was significantly influenced by loading condition, slenderness, and confinement technique. The use of full CFRP wrapping improved confinement effectiveness, reducing brittle behavior and enhancing the structural performance under both concentric and eccentric compression loading. Accordingly, the main conclusions drawn from this study are summarized as follows:

- The strength of the short square RC columns with inadequate interior ties under concentric loading was substantially lower than that of the corresponding columns with adequate interior ties by approximately 27%. In contrast, the slender columns showed only a small decrease of approximately 1% under the same loading condition, indicating that slenderness-related stability effects had a greater influence on the peak load than the adequacy of the interior ties. However, at peak load, both the short and slender columns with inadequate interior ties failed in a brittle manner.
- The effect of inadequate interior ties on the strength of both the short and slender square RC columns under eccentric loading conditions was less pronounced than under concentric loading. The reduction of strength was around 11% for the short columns and 4% in the case of slender columns. Moreover, brittle failure was not observed under the same loading conditions.
- The short square RC columns exhibited limited variation in lateral deformation response, regardless of confinement or loading conditions. By contrast, the effect was more pronounced in the slender columns.
- In both short and slender square RC columns subjected to eccentric loading, the displacement ductility was only slightly influenced by inadequate interior ties compared with that under the concentric loading condition.
- The use of full CFRP wrapping for square RC columns with inadequate interior ties improved the strength and displacement ductility of both short and slender columns under concentric and eccentric loading conditions. In addition, CFRP wrapping prevented brittle failure at peak load and proved to be an effective strengthening technique for compensating for inadequate interior ties in RC columns. The improvement in ductility was more pronounced in the short columns than in the slender columns.
- Regardless of concentric or eccentric loading conditions, the concrete compressive strain at peak load of square columns with inadequate interior ties strengthened with full CFRP wrapping was higher than that of the corresponding unconfined columns with inadequate interior ties. The improvement was more pronounced in the short columns, whereas the slender columns exhibited lower enhancement, indicating that the contribution of CFRP confinement to the measured concrete strain was reduced by slenderness-related deformation and stability effects.
- The effect of slenderness on the strength of square RC columns depends on the confinement condition and type of loading. The reference columns with adequate interior ties experienced significant strength reductions with increasing slenderness, whereas only small differences were observed in the strength of the columns with inadequate interior ties. Furthermore, CFRP confinement reduced the slenderness effect in concentric compression. However, under eccentric loading, all slender RC columns exhibited lower strength and greater sensitivity to lateral deformation and instability than corresponding short columns.
- The strength of both the short and slender square RC columns was significantly reduced under eccentric loading, regardless of the confinement condition. However, in the short columns with inadequate interior ties, CFRP confinement partially mitigated the reduction in strength. In contrast, all slender columns were more sensitive to eccentric compression

because of the increased bending action and instability effects. Although CFRP confinement improved the strength of the slender columns, the influence of slenderness-related deformation and stability effects remained significant.

- When CFRP strengthening is applied to slender RC columns with inadequate interior ties, the influence of column slenderness should be considered during design and assessment in addition to the confinement effect provided by CFRP.

References

[1] Richart FE, Brandtzaeg A, Brown RL. A study of the failure of concrete under combined compressive stresses. Urbana, IL: 1928.

[2] Sheikh SA, Uzumeri SM. Strength and ductility of tied concrete columns. Journal of the Structural Division 1980;106:1079–102. https://doi.org/10.1061/JSDEAG.0005416.

[3] Mander JB, Priestley MJN, Park R. Theoretical stress-strain model for confined concrete. Journal of Structural Engineering 1988;114:1804–26. https://doi.org/10.1061/(ASCE)0733-9445(1988)114:8(1804).

[4] Saatcioglu M, Salamat AH, Razvi SR. Confined columns under eccentric loading. Journal of Structural Engineering 1995;121:1877–83. https://doi.org/10.1061/(ASCE)0733-9445(1995)121:11(1547).

[5] Somma G, Pieretto A. Confinement effects on high strength concrete under axial load: Evaluation of international standards prescriptions. Materials and Structures/Materiaux et Constructions 2016;49:57–69. https://doi.org/10.1617/s11527-014-0474-5.

[6] Ma J, Yu L, Li B, Yu B. Stress–strain model for confined concrete in rectangular columns with corroded transverse reinforcement. Eng Struct 2022;267:114710. https://doi.org/10.1016/j.engstruct.2022.114710.

[7] Benedetti F, Bairán JM. Model for the assessment of rectangular reinforced concrete columns with limited confinement details. Results in Engineering 2025;27:105985. https://doi.org/10.1016/j.rineng.2025.105985.

[8] Ozmen HB, Inel M. Effect of concrete strength and detailing properties on seismic damage for RC structures. Research and Design 2024;1:1–11. https://doi.org/10.17515/rede2024-005en1124rs.

[9] Mahboubi S, Shiravand MR. Failure assessment of skew RC bridges with FRP piers based on damage indices. Eng Fail Anal 2019;99:153–68. https://doi.org/10.1016/j.engfailanal.2019.02.010.

[10] Naqe AW, Al-zuhairi AH. Strengthening of RC beam with large square opening using CFRP. Journal of Engineering 2020;26:123–34. https://doi.org/10.31026/j.eng.2020.10.09.

[11] Yan ZW, Bai YL, Ozbakkaloglu T, Gao WY, Zeng JJ. Axial impact behavior of Large-Rupture-Strain (LRS) fiber reinforced polymer (FRP)-confined concrete cylinders. Compos Struct 2021;276. https://doi.org/10.1016/j.compstruct.2021.114563.

[12] Shaikh FUA, Alishahi R. Behaviour of CFRP wrapped RC square columns under eccentric compressive loading. Structures 2019;20:309–23. https://doi.org/10.1016/j.istruc.2019.04.012.

[13] Yaman S. Calibration of a general analytical model for the debonding strength of NSM-CFRP strip-concrete joints using particle swarm optimization. Research on Engineering Structures and Materials 2025;11:2701–14. https://doi.org/10.17515/resm2025-1131an0905rs.

[14] Ayazian R, Abdolhosseini M, Firouzi A, Li CQ. Reliability-based optimization of external wrapping of CFRP on reinforced concrete columns considering decayed diffusion. Eng Fail Anal 2021;128:105592. https://doi.org/10.1016/j.engfailanal.2021.105592.

[15] Van Cao V, Pham SQ. Comparison of CFRP and GFRP wraps on reducing seismic damage of deficient reinforced concrete structures. International Journal of Civil Engineering 2019;17:1667–81. https://doi.org/10.1007/s40999-019-00429-y.

[16] Samy K, Fouda MA, Fawzy A, Elsayed T. Enhancing the effectiveness of strengthening RC columns with CFRP sheets. Case Studies in Construction Materials 2022;17. https://doi.org/10.1016/j.cscm.2022.e01588.

[17] Al-Nimry HS, Al-Rabadi RA. Axial–flexural interaction in FRP-wrapped RC columns. Int J Concr Struct Mater 2019;13. https://doi.org/10.1186/s40069-019-0366-8.

[18] Tafsirojjaman T, Ur Rahman Dogar A, Liu Y, Manalo A, Thambiratnam DP. Performance and design of steel structures reinforced with FRP composites: A state-of-the-art review. Eng Fail Anal 2022;138:106371. https://doi.org/10.1016/j.engfailanal.2022.106371.

[19] Sadeghian P, Fillmore B. Strain distribution of basalt FRP-wrapped concrete cylinders. Case Studies in Construction Materials 2018;9. https://doi.org/10.1016/j.cscm.2018.e00171.

[20] Castro Quispe VJ, de Diego Villalón A, León González FJ, Martínez de Mingo S, Echevarría Giménez L. Evaluating the effectiveness of CFRP confinement: New model and simplified estimation of ductility improvement. Structures 2024;70:107825. https://doi.org/10.1016/j.istruc.2024.107825.

[21] Al-Ahmed AHA, Al-Jburi MHM. Behavior of reinforced concrete deep beams strengthened with carbon fiber reinforced polymer strips. Journal of Engineering 2016;22:37–53. https://doi.org/10.31026/j.eng.2016.08.03.
[22] Abdulsattar AW, Al-Baghdadi HA. Experimental and numerical study of CFRP-confined square concrete columns under axial compression. Journal of Engineering 2020;26:141–60. https://doi.org/10.31026/j.eng.2020.04.10.
[23] Mai AD, Sheikh MN, Hadi MNS. Investigation on the behaviour of partial wrapping in comparison with full wrapping of square RC columns under different loading conditions. Constr Build Mater 2018;168:153–68. https://doi.org/10.1016/j.conbuildmat.2018.02.003.
[24] Mercimek Ö, Ghoroubi R, Anil Ö, Çakmak C, Özdemir A, Kopraman Y. Strength, ductility, and energy dissipation capacity of RC column strengthened with CFRP strip under axial load. Mechanics Based Design of Structures and Machines 2020;51:961–79. https://doi.org/10.1080/15397734.2020.1860772.
[25] Saleh E, Tarawneh A, Almasabha G, Momani Y. Slenderness limit of FRP-confined rectangular concrete columns. Structures 2022;38:435–47. https://doi.org/10.1016/j.istruc.2022.02.030.
[26] Narule GN, Bambole AN. An experimental study on axial behavior of CFRP-strengthened RC rectangular columns with variable slenderness ratio. Asian Journal of Civil Engineering 2021;22:263–75. https://doi.org/10.1007/s42107-020-00312-5.
[27] Ali FA, Hasan QA, Mohammed DH. Strengthening of recycled aggregate concrete slender column with CFRP. E3S Web of Conferences, vol. 427, EDP Sciences; 2023, p. 02015. https://doi.org/10.1051/e3sconf/202342702015.
[28] Al-Sherrawi MH, Salman HM, Mohammed SD. Analytical and theoretical development of load-moment interaction diagrams of rectangular CFRP-RC columns. Engineering, Technology and Applied Science Research 2025;15:25178–91. https://doi.org/10.48084/etasr.12059.
[29] Mousa AM, Al Zaidee SR. Numerical study of CFRP-strengthened square RC columns under axial compression with initial geometric imperfections. Journal of Engineering 2026;32:93–115. https://doi.org/10.31026/j.eng.2026.05.05.
[30] ACI Committee 318. Building code for structural concrete—Code requirements and commentary (ACI CODE-318-25). Farmington Hills, MI: American Concrete Institute; 2025.
[31] ACI Committee 440. Design and construction of externally bonded fiber-reinforced polymer (FRP) systems for strengthening concrete structures—Guide (ACI PRC-440.2-23). Farmington Hills, MI: American Concrete Institute; 2023.
[32] Fosroc. Nitowrap CW: High performance, high strength carbon fibre system for structural reinforcement of concrete. 2019.
[33] Sika Services AG. Sikadur-330: 2-component epoxy impregnation resin—Product data sheet. 2020.
[34] Wight JK. Reinforced concrete: Mechanics and design. 8th ed. Pearson; 2021.
[35] Darwin David, Dolan CW. Design of concrete structures. 16th ed. McGraw-Hill Education; 2021.
[36] Ghoroubi R, Mercimek Ö, Özdemir A, Anil Ö. Experimental investigation of damaged square short RC columns with low slenderness retrofitted by CFRP strips under axial load. Structures 2020;28:170–80. https://doi.org/10.1016/j.istruc.2020.08.068.